

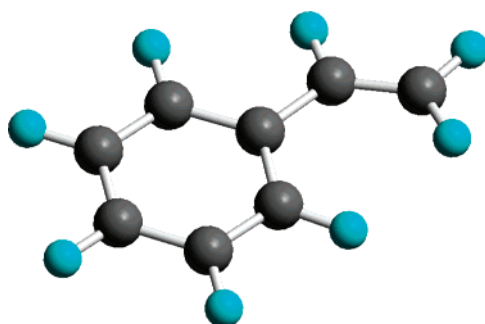
Reaction Dynamics on the Formation of Styrene: A Crossed Molecular Beam Study of the Reaction of Phenyl Radicals with Ethylene

F. Zhang, X. Gu, Y. Guo, and R. I. Kaiser*

Department of Chemistry, University of Hawai'i at Manoa, Honolulu, Hawaii 96822

ralfk@hawaii.edu

Received May 17, 2007



The reaction dynamics of phenyl radicals (C_6H_5) with ethylene (C_2H_4) and D4-ethylene (C_2D_4) were investigated at two collision energies of 83.6 and 105.3 kJ mol^{-1} utilizing a crossed molecular beam setup. The experiments suggested that the reaction followed indirect scattering dynamics via complex formation and was initiated by an addition of the phenyl radical to the carbon-carbon double bond of the ethylene molecule forming a $C_6H_5CH_2CH_2$ radical intermediate. Under single collision conditions, this short-lived transient species was found to undergo unimolecular decomposition via atomic hydrogen loss through a tight exit transition state to synthesize the styrene molecule ($C_6H_5C_2H_3$). Experiments with D4-ethylene verified that in the corresponding reaction with ethylene the hydrogen atom was truly emitted from the ethylene unit but not from the phenyl moiety. The overall reaction to form styrene plus atomic hydrogen from the reactants was found to be exoergic by $25 \pm 12 \text{ kJ mol}^{-1}$. This study provides solid evidence that in combustion flames the styrene molecule, a crucial precursor to form polycyclic aromatic hydrocarbons (PAHs), can be formed within a single neutral-neutral collision, a long-standing theoretical prediction which has remained to be confirmed by laboratory experiments under well-defined single collision conditions for the last 50 years.

Introduction

Polycyclic aromatic hydrocarbons (PAHs)¹ and related molecules such as partially (de)hydrogenated^{2–4} and ionized PAHs^{5,6} have attracted substantial interest from the astrochemical^{7–9} and

combustion communities during the last century.¹⁰ In interstellar space, PAH-like species have been linked to the unidentified infrared (UIR) emission bands observed in the range of 3–14 μm ($3300\text{--}700 \text{ cm}^{-1}$).¹¹ They have been further considered as a carrier of the diffuse interstellar bands (DIBs),¹² discrete absorption features superimposed on the interstellar extinction

(1) Weisman, J. L.; Mattioda, A.; Lee, T. J.; Hudgins, D. M.; Allamandola, L. J.; Bauschlicher, C. W., Jr.; Head-Gordon, M. *Phys. Chem. Chem. Phys.* **2005**, *7*, 109–118.

(2) Bernstein, M. P.; Sandford, S. A.; Allamandola, L. J. *Astrophys. J.* **1996**, *472*, L127–L130.

(3) Mendoza-Gomez, C. X.; Groot, M. S. d.; Greenberg, J. M. *Astron. Astrophys.* **1995**, *295*, 479–486.

(4) Papas, B. N.; Wang, S.; DeYonker, N. J.; Woodcock, H. L.; Schaefer, H. F., III. *J. Phys. Chem. A* **2003**, *107*, 6311–6316.

(5) Ekern, S. P.; Marshall, A. G.; Szczepanski, J.; Vala, M. *J. Phys. Chem. A* **1998**, *102*, 3498–3504.

(6) Hudgins, D. M.; Bauschlicher, C. W., Jr.; Allamandola, L. J.; Fetzer, J. C. *J. Phys. Chem. A* **2000**, *104*, 3655–3669.

(7) Ehrenfreund, P. *Science* **1999**, *283*, 1123–1124.

(8) Pendleton, Y. J.; Allamandola, L. J. *Astrophys. J., Suppl. Ser.* **2002**, *138*, 75–98.

(9) Salama, F.; Allamandola, L. J. *Astrophys. J.* **1992**, *395*, 301–306.

(10) Kazakov, A.; Frenklach, M. *Combust. Flame* **1998**, *112*, 270–274.

(11) Peeters, E.; Mattioda, A. L.; Hudgins, D. M.; Allamandola, L. J. *Astrophys. J.* **2004**, *617*, L65–L68.

curve,¹³ ranging from the blue part of the visible (400 nm) to the near-infrared (1.2 μm).¹⁴ Whereas in the interstellar medium PAH-like species are crucial to understand the astrochemical and astrobiological evolution of carbon-rich environments such as circumstellar envelopes of carbon-rich stars IRC+10216 and planetary nebulae, they on Earth are considered as toxic byproducts in combustion processes of fossil fuel. Here, the growth mechanisms of PAHs and their role in the formation of soot particles have been investigated from the combustion, medical, and environmental points of view. Considering a yearly emission rate of 1.6 million tons in combustion processes,¹⁵ PAHs and soot are severe air and marine pollutants,^{16,17} contribute to global warming,¹⁸ and are considered as airborne toxic chemicals because of their mutagenic and carcinogenic character. Consequently, a quantitative understanding of the formation of PAHs is essential to develop clean combustion devices and also to comprehend the astrochemical as well as the astrobiological evolution of the interstellar medium.

Contemporary reaction networks mimicking PAH formation in combustion flames^{19–21} and in the interstellar medium²² concur that the phenyl radical (C_6H_5) in its $^2\text{A}_1$ electronic ground state presents the most important transient species to trigger the formation of PAHs.^{10,23} The phenyl radical itself has been scavenged as a methylthioether in flames.²⁴ Recently, the phenyl radical was also assigned via its ionization potential in sooting hydrocarbon flames utilizing tunable vacuum ultraviolet light from synchrotron sources.^{25,26} Therefore, both the matrix and the ionization studies demonstrated explicitly the existence of phenyl radicals in high-temperature hydrocarbon flames. Because of the crucial importance of the phenyl radical in combustion processes and extraterrestrial environments, a multitude of kinetic and spectroscopic investigations have been carried out in the past. The most precise measurements of rate constants of phenyl radical reactions with alkenes and alkynes have been taken via cavity ring-down spectroscopy,^{27–36} these

data show rate constants at temperature up to 1500 K ranging between 10^{-11} and 10^{-12} $\text{cm}^3 \text{s}^{-1}$. These studies show also activation energies ranging between 5 and 45 kJ mol^{-1} upon addition of the radical to olefines and alkynes.^{32,37} But despite valuable kinetic data, the reaction products, which are crucial to know for a detailed chemical modeling of combustion processes and PAH formation in circumstellar shells of carbon stars, were rarely probed.

Considering the simplest reaction of a phenyl radical with an olefin, Stein et al. conducted bulk experiments and carried out low-pressure pyrolysis studies on the reaction of phenyl radicals with ethylene in the range of 1000–1300 K.²⁸ The authors inferred the styrene molecule ($\text{C}_6\text{H}_5\text{C}_2\text{H}_3$) as a reaction product. However, bulk experiments have shown to be problematic since they are often influenced by wall effects.^{38,39} Further, pyrolysis studies cannot provide detailed information on the reaction dynamics involved. On the basis of quantum chemical and statistical calculations, Lin et al. proposed that the reaction involved an initial addition of the phenyl radical to the carbon–carbon double bond of the ethylene molecule via a phenylethyl radical, $\text{C}_6\text{H}_5\text{C}_2\text{H}_4$, followed by atomic hydrogen elimination.³⁷ Note that this radical intermediate is utilized in polymer chemistry as a model compound to understand the region selectivity of polystyrene radicals.^{40–42} Also, the phenylethyl radical is formed during the in vivo oxidation of the drug phenylethylhydrazine and is often utilized to understand the metabolism of hydrazine and analogues compounds as well as DNA damage by carbon-centered radicals.^{43–46}

Despite the central role of the phenyl–ethylene reaction in the formation of PAHs, and the role of potential phenylethyl radical intermediates in polymer science and medicinal chemistry, the theoretical investigations have never been verified experimentally under single collision conditions, i.e., experimental conditions in which the outcome of a single collision can be observed without any wall effects. Here, we present the very first crossed molecular beam study of the reaction of the phenyl radical, C_6H_5 , with ethylene, C_2H_4 , as the simplest representative of an olefinic reactant molecule to synthesize

(12) Romanini, D.; Biennier, L.; Salama, F.; Kachanov, A.; Allamandola, L. J.; Stoeckel, F. *Chem. Phys. Lett.* **1999**, *303*, 165–170.

(13) Duley, W. W. *Faraday Discuss.* **2006**, *133*, 415–425.

(14) Van der Zwet, G. P.; Allamandola, L. J. *Astron. Astrophys.* **1985**, *146*, 76–80.

(15) Seinfeld, J. H.; Pankow, J. F. *Annu. Rev. Phys. Chem.* **2003**, *54*, 121–140.

(16) Finlayson-Pitts, B. J.; Pitts, J. N., Jr. *Science* **1997**, *276*, 1045–1052.

(17) Hylland, K. J. *Toxicol Environ. Health A* **2006**, *69*, 109–123.

(18) Violi, A.; Venkatnathan, A. *J. Chem. Phys.* **2006**, *125*, 054302/054301–054302/054308.

(19) Appel, J.; Bockhorn, H.; Frenklach, M. *Combust. Flame* **2000**, *121*, 122–136.

(20) Frenklach, M. *Phys. Chem. Chem. Phys.* **2002**, *4*, 2028–2037.

(21) Richter, H.; Howard, J. B. *Phys. Chem. Chem. Phys.* **2002**, *4*, 2038–2055.

(22) Frenklach, M.; Feigelson, E. D. *Astrophys. J.* **1989**, *341*, 372–384.

(23) McMahon, R. J.; McCarthy, M. C.; Gottlieb, C. A.; Dudek, J. B.; Stanton, J. F.; Thaddeus, P. *Astrophys. J.* **2003**, *590*, L61–L64.

(24) Hausmann, M.; Homann, K. H. *Ber. Bunsen-Ges.* **1990**, *94*, 1308–1312.

(25) Hansen, N.; Klippenstein, S. J.; Miller, J. A.; Wang, J.; Cool, T. A.; Law, M. E.; Westmoreland, P. R.; Kasper, T.; Kohse-Hoeinghaus, K. *J. Phys. Chem. A* **2006**, *110*, 4376–4388.

(26) Hansen, N.; Klippenstein, S. J.; Taatjes, C. A.; Miller, J. A.; Wang, J.; Cool, T. A.; Yang, B.; Yang, R.; Wei, L.; Huang, C.; Wang, J.; Qi, F.; Law, M. E.; Westmoreland, P. R. *J. Phys. Chem. A* **2006**, *110*, 3670–3678.

(27) Duncan, F. J.; Trotman-Dickenson, A. F. *J. Chem. Soc.* **1962**, 4672–4676.

(28) Fahr, A.; Stein, S. E. *Symp. (Int.) Combust., [Proc.]* **1989**, *22nd*, 1023–1029.

(29) Herzler, J.; Frank, P. *Ber. Bunsen-Ges.* **1992**, *96*, 1333–1338.

(30) Wang, R.; Cadman, P. *Combust. Flame* **1998**, *112*, 359–370.

(31) Yu, T.; Lin, M. C. *J. Phys. Chem.* **1995**, *99*, 8599–8603.

(32) Yu, T.; Lin, M. C. *Combust. Flame* **1995**, *100*, 169–176.

(33) Richter, H.; Mazyar, O. A.; Sumathi, R.; Green, W. H.; Howard, J. B.; Bozzelli, J. W. *J. Phys. Chem. A* **2001**, *105*, 1561–1573.

(34) Park, J.; Nam, G. J.; Tokmakov, I. V.; Lin, M. C. *J. Phys. Chem. A* **2006**, *110*, 8729–8735.

(35) Tokmakov, I. V.; Park, J.; Lin, M. C. *ChemPhysChem* **2005**, *6*, 2075–2085.

(36) Park, J.; Wang, L.; Lin, M. C. *Int. J. Chem. Kinet.* **2003**, *36*, 49–56.

(37) Tokmakov, I. V.; Lin, M. C. *J. Phys. Chem. A* **2004**, *108*, 9697–9714.

(38) Hofmann, J.; Zimmermann, G.; Guthier, K.; Hebgren, P.; Homann, K.-H. *Liebigs Ann.* **1995**, 631–636.

(39) Sorkhabi, O.; Qi, F.; Rizvi, A. H.; Suits, A. G. *J. Am. Chem. Soc.* **2001**, *123*, 671–676.

(40) Bevington, J. C.; Cywar, D. A.; Huckerby, T. N.; Senogles, E.; Tirrell, D. A. *Eur. Polym. J.* **1990**, *26*, 871–875.

(41) Jenkins, A. D. *Polymer* **1999**, *40*, 7045–7058.

(42) Skene, W. G.; Scaiano, J. C.; Yap, G. P. A. *Macromolecules* **2000**, *33*, 3536–3542.

(43) Justo, G. Z.; Livotto, P. R.; Duran, N. *Free Radical Biol. Med.* **1995**, *19*, 431–440.

(44) Leite, L. C. C.; Augusto, O. *Arch. Biochem. Biophys.* **1989**, *270*, 560–572.

(45) Ortiz de Montellano, P. R.; Watanabe, M. D. *Mol. Pharmacol.* **1987**, *31*, 213–219.

(46) Yamamoto, K.; Kawanishi, S. *Chem. Res. Toxicol.* **1992**, *5*, 440–446.

styrene (phenylethylene) $C_6H_5C_2H_3$, plus atomic hydrogen via $[C_8H_9]^*$ intermediate(s). By deriving the underlying reaction dynamics and the reaction mechanism, this helps not only to gain a systematic understanding of the formation of PAHs in combustion flames and in the interstellar medium but also assists to conduct organic radical reactions (here: radical substitution reactions) on the most fundamental, microscopic level.

Methodology

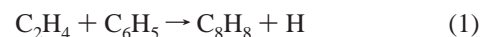
The crossed molecular beam method presents a powerful experimental technique to investigate the reaction dynamics of important combustion reactions.⁴⁷ The networks of chemical processes occurring in combustion flames consist of a series of elementary reactions, most of which are bimolecular collisions between a radical or atom and a closed shell species. A detailed experimental knowledge of the elementary processes involved at a fundamental microscopic level is therefore desirable, even if we want simply to assess the nature of the primary reaction products. Experiments under single collision conditions are essential to achieve this because in a binary collision involving phenyl (C_6H_5) radicals and a generic hydrocarbon, RH, where an intermediate is formed, i.e., $C_6H_5 + RH \rightarrow [C_6H_5RH]^* \rightarrow C_6H_5R + H$, a phenyl radical reacts solely with one single hydrocarbon molecule and the stabilization of the $[C_6H_5RH]^*$ intermediate and/or successive reaction of the primary products will be eliminated. Only this requirement can guarantee that the real primary reaction products are identified. In contrast to bulk experiments, where the reactants are mixed, the main advantage of a crossed beam experiment is the capability to confine the reactants (here phenyl and ethylene molecules) in separate, supersonic beams; this implies that the radicals will collide only with the molecules of a second beam at a specific collision energy and crossing angle, therefore ensuring the observation of the consequences of well-defined molecular collision.

To detect the product, our machine incorporates a triply differentially pumped, *universal* quadrupole mass spectrometric detector coupled to an electron impact ionizer operating at extreme ultrahigh vacuum conditions down to 10^{-13} Torr. Here, any reactively species scattered from the collision center after a single collision event took place can be ionized in the electron impact ionizer, and in principle it is possible to determine the mass (and the gross formula) of all the products of a bimolecular reaction by varying the mass-to-charge ratio, m/z , in the mass filter. Since the detector is rotatable within the plane defined by both beams, this detector makes it possible to map out the angular and velocity distributions of the scattered products. Measuring the time-of-flight (TOF) of the products from the interaction region over a finite flight distance allows extraction of the product translational energy and angular distributions in the center-of-mass reference frame. This provides direct insights into the nature of the chemical reaction (direct vs indirect), intermediates involved, the reaction product(s), their branching ratios, and in some cases the preferential rotational axis of the fragmenting complex(es) and the disposal of excess energy into the products' internal degrees of freedom as a function of scattering angle and collision energy (cf. Experimental Section).

Results and Discussion

Laboratory Data. In the crossed molecular beam experiment of phenyl radicals with ethylene, the reactive scattering signal

was monitored at mass-to-charge ratios, m/z , from $m/z = 104$ ($C_8H_8^+$) to 102 ($C_8H_6^+$) at both collision energies (Figure 1a). Most important, within this mass range, the TOF spectra are, after scaling, superimposable. This indicates that ion counts at $m/z = 103$ and 102 originate from dissociative ionization of the C_8H_8 product in the electron impact ionizer. Also, the interpretation of the TOF data suggests that only the atomic hydrogen replacement channel is open within this mass regime to form species with the molecular formula C_8H_8 (eq 1); the molecular hydrogen replacement channels are closed. We would like to point out that we also detected ion counts at $m/z = 105$. The corresponding TOF is superimposable with the one taken at $m/z = 104$; in addition, the intensity of signal at $m/z = 105$ is only about $10 \pm 2\%$ of the ion count rate at $m/z = 104$. Therefore, we can conclude that ions at $m/z = 105$ originate from the ionized $^{13}CC_7H_8$ reaction product but, within our error limits, not from a C_8H_9 adduct.



Next, we would like to answer the question whether the hydrogen atom originated from the phenyl radical or from the ethylene reactant. To gain insight into this topic, we carried out a crossed beam experiment of the phenyl radical (77 amu) with D4-ethylene (32 amu). If a hydrogen atom elimination takes place from the phenyl group, a signal should be detected at $m/z = 108$ ($C_8H_4D_4^+$); an atomic deuterium loss pathway (from D4-ethylene) should yield $m/z = 107$ ($C_8H_5D_3^+$). It is important to stress that $m/z = 107$ can in principle originate, if formed, also from dissociative ionization of $C_8H_4D_4$ in the electron impact ionizer of the detector. In the crossed beam experiment at the corresponding center-of-mass angles, we observed a strong signal at $m/z = 107$ ($C_8H_5D_3^+$) (Figure 1b); a small signal at $m/z = 108$, which is superimposable on the TOF recorded at $m/z = 107$, can be attributed to ($^{13}CC_7H_5D_3^+$). These findings indicate that only a deuterium atom is emitted from the D4-ethylene reactants (eq 2). Consequently, we can conclude that in the crossed beam reactions of the phenyl radical with ethylene, the hydrogen atom originated from the ethylene reactant but not from the phenyl radical. Finally, we probed to what extent a hydrogen abstraction pathway forming benzene (C_6H_6 ; $m/z = 78$) plus vinyl (C_2H_3) is involved in the dynamics. When we monitored $m/z = 78$, we detected strong interference from elastically scattered $^{13}CC_5H_5$ radicals at $m/z = 78$. To bypass this interference, we tried to monitor the deuterium abstraction pathway to form D1-benzene (C_6H_5D) in the reaction of phenyl with D4-ethylene. At $m/z = 79$, no background molecules interfered; however, we were unable to detect any reactive scattering signal. This led us to the conclusion that in the reactions of phenyl with ethylene and D4-ethylene, only the phenyl versus atomic hydrogen/deuterium pathways are open.



Center-of-Mass Translational Energy, $P(E_T)$ s, and Angular Distributions, $T(\theta)$ s. Since the TOF spectra verified the formation of C_8H_8 isomer(s), we attempt now to unravel the underlying reaction dynamics. This assists the extraction of reaction energies and gains additional data on potential entrance and exit barriers of this reaction. Most importantly, the dynamics aid the assignment of the product isomer(s) and help to infer the intermediate(s) involved. At both higher and lower collision

(47) Kaiser, R. I.; Balucani, N. *Acc. Chem. Res.* **2001**, *34*, 699–706.

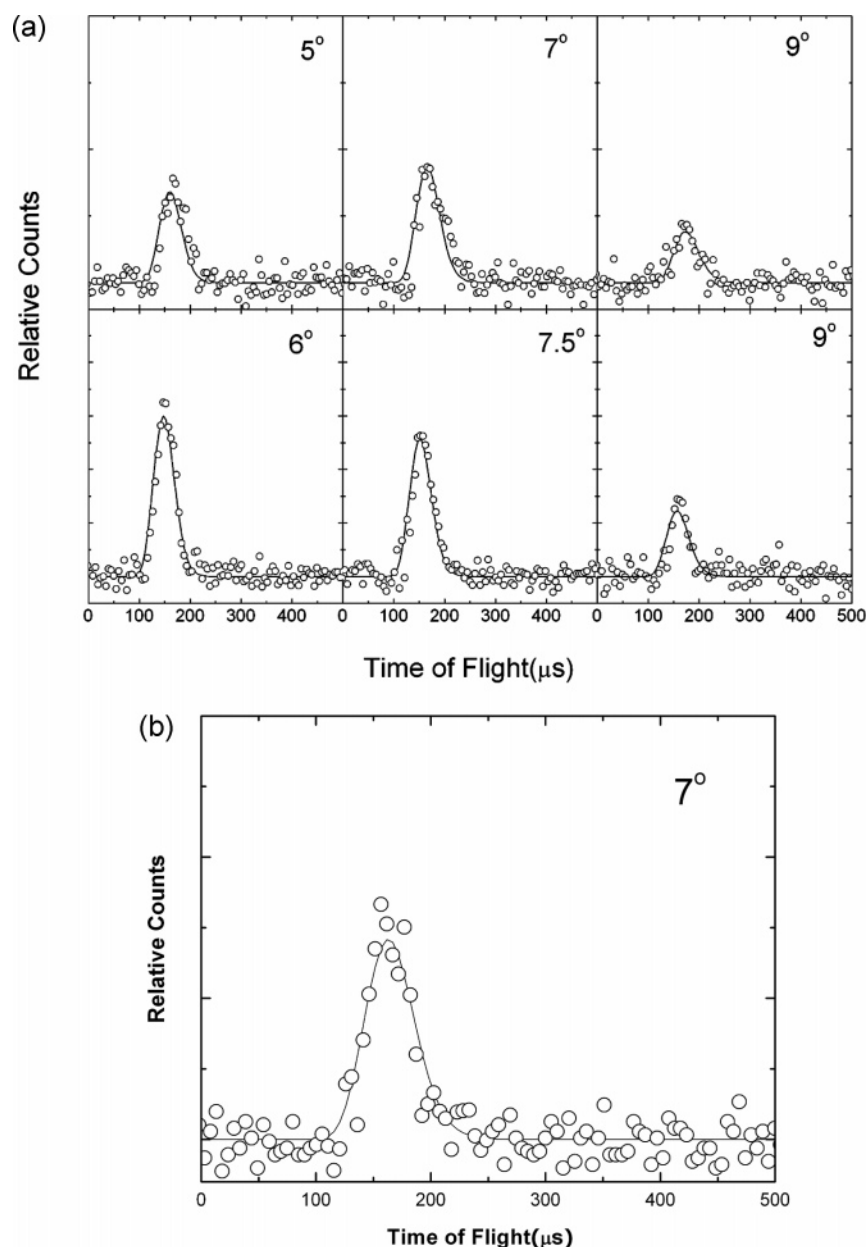
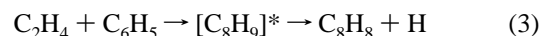


FIGURE 1. (a) Selected time-of-flight data recorded at mass-to-charge ratio (m/z) of 104 ($C_8H_8^+$) for two collision energies of 83.6 (upper row) and 105.3 kJ mol^{-1} (lower row). The open circles are the experimental data, the solid lines the fits. The quadrupole mass filter was set at a constant $m/z = 104$; the mass spectrometer was then operated in the time-of-flight (TOF) mode to record the arrival time of the ionized products of $m/z = 104$. (b) Time-of-flight spectrum recorded at mass-to-charge ratio (m/z) of 107 ($C_8H_5D_3^+$). The open circles are the experimental data, the solid lines the fits. The quadrupole mass filter was set at a constant $m/z = 107$; the mass spectrometer was then operated in the time-of-flight (TOF) mode to record the arrival time of the ionized products of $m/z = 107$.

energies, the TOF spectra (Figure 1) and laboratory angular distributions (Figure 2) could be fit with only one channel at each collision energy. The center-of-mass translational energy, $P(E)$ s, and angular distributions, $T(\theta)$ s, are shown in Figure 3. The center-of-mass angular distributions at both collision energies depict, within the error limits, intensity over the complete range from 0° to 180° ; this finding indicates that the reaction dynamics are indirect and involve the formation of C_8H_9 intermediate(s), $[C_8H_9]^*$, before the latter decompose via atomic hydrogen elimination to the C_8H_8 product(s) (eq 3). Second, the $T(\theta)$ s depict a pronounced forward scattering: the flux of the heavy reaction product at 0° is enhanced compared to 180° . This result, combined with the single channel fit of the laboratory data, suggests that the lifetime(s) of the decomposing

reaction intermediate(s) is(are) shorter than the rotational period and that the reaction likely proceeds via an oscillating complex.⁴⁸ It is important to stress that because of the kinematics of the reactions, i.e., a narrow angular range in the laboratory frame of the reactively scattered heavy product of only 10° (Figure 2), the $T(\theta)$ s do not change much when the collision energy is raised from 83.6 to 105.3 kJ mol^{-1} .



The translational energy distributions contribute to the collection of additional information on the reaction dynamics.

(48) Miller, W. B.; Safron, S. A.; Herschbach, D. R. *Discuss. Faraday Soc.* **1967**, No. 44, 108–122.

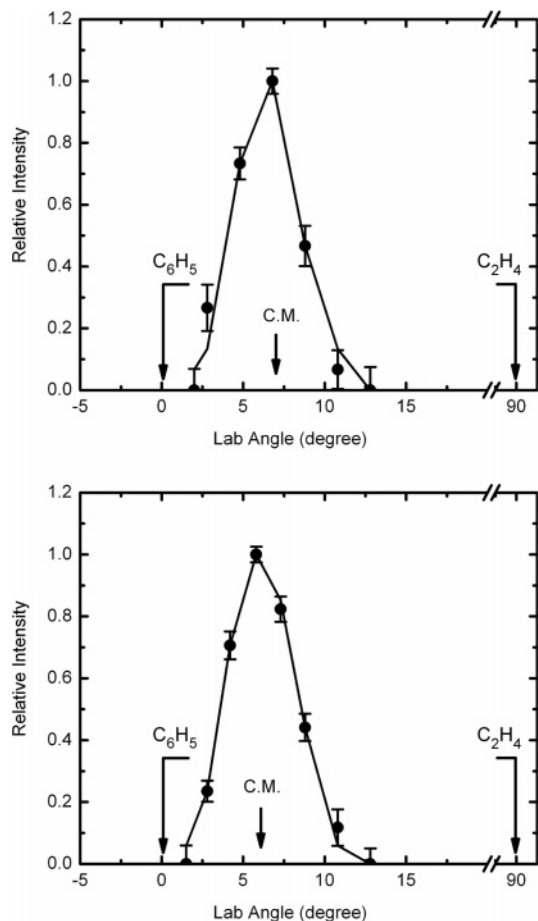
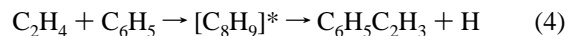


FIGURE 2. Laboratory angular distributions recorded at mass-to-charge ratio (m/z) of 104 ($C_8H_8^+$) for two collision energies of 83.6 (upper) and 105.3 kJ mol^{-1} (lower).

Both distributions show maxima around 10–25 kJ mol^{-1} . This likely indicates a tight exit transition state when the C_8H_9 intermediate(s) fragment to the final C_8H_8 products plus atomic hydrogen.⁴⁹ On the basis of the principle of microscopic reversibility of a chemical reaction, the reversed reaction of hydrogen addition to the C_8H_8 product is therefore expected to have an entrance barrier.⁵⁰ In addition, the high-energy cut-offs of the translational energy distributions resemble the sum of the absolute of the reaction exoergicity plus the relative collision energy. By extraction the latter and averaging over both experiments, the data suggest that the reaction is exoergic by $25 \pm 12 \text{ kJ mol}^{-1}$. These data correlate nicely with the computed exoergicity of $30 \pm 8 \text{ kJ mol}^{-1}$ ³⁷ and the energy derived from the NIST database of $-26 \pm 9 \text{ kJ mol}^{-1}$ ⁵¹ and from ref 52 of $-21 \pm 3 \text{ kJ mol}^{-1}$ to form the styrene isomer (phenylacetylene; $C_6H_5C_2H_3$) plus atomic hydrogen (eq 4). On the basis of this, we can extract the fraction of available energy channeled into the translational degrees of freedom of the reactants to be about $30 \pm 3\%$. This order-of-magnitude is

consistent with the complex-forming reaction mechanism.⁵³ Finally, best fits of the TOF data and laboratory angular distributions were achieved by adjusting the threshold energy within the fitting routine to be in the range of 10–35 kJ mol^{-1} . This compares favorably with an activation energy of 9.6 kJ mol^{-1} as derived by Lin et al.³⁷



Discussion

Having identified the styrene molecule as the product in the reaction of phenyl radicals with ethylene, we are attempting now to derive the underlying reaction mechanism. The experimental results suggest that the phenyl radical adds with its radical center to the carbon–carbon double bond of the ethylene molecule forming a C_8H_9 doublet radical intermediate (Figure 4; **ii**). Recall that the threshold energy points to an entrance barrier in the range of 10–35 kJ mol^{-1} . Also, the shapes of the center-of-mass angular distributions are indicative of complex-forming, ‘indirect’ scattering dynamics as proposed here. At both collision energies, the lifetime of the decomposing intermediate was found to be much shorter than the rotational period. The initial collision complex decomposed via atomic hydrogen emission through a tight exit transition state located 10–20 kJ mol^{-1} above the separated products. In other words, the reversed reaction of a hydrogen atom addition to the C2 atom of the vinyl group has an entrance barrier. This reaction mechanism correlates with a previous theoretical study.⁴⁰ Here, the authors proposed that the phenyl radical added with its unpaired electron to the ethylene molecule via a barrier of about 10 kJ mol^{-1} leading to an intermediate **ii** which is stabilized by 152 kJ mol^{-1} . This relatively shallow potential energy well could result in the relatively short lifetime of the reaction intermediate as deduced from the center-of-mass angular distributions. The computations suggested further that this intermediate ejects a hydrogen atom via a tight exit transition state located 25 kJ mol^{-1} above the styrene and atomic hydrogen products. Most importantly, both our phenyl–ethylene experiments and the computations are supported by the sole detection of the atomic deuterium pathway observed in the crossed beams reaction of D4-ethylene with the phenyl radical: on the basis of the suggested reaction pathways and the computed surface (Figure 4), the phenyl group stays intact during the reaction. Recall that the indirect nature of the reaction mechanisms as inferred from the center-of-mass angular distributions is similar, for example, as found in the reaction of cyano radicals (CN) with ethylene studied previously under single collision conditions.⁴⁷ Finally, the experiments confirm the sole existence of the atomic hydrogen loss pathway in the phenyl–ethylene system and the absence of the hydrogen abstraction pathway to form benzene plus the vinyl radical.

It should be noted that the computations also indicated the possibility of hydrogen migrations in the initial adduct **ii** to **ii2** and **ii3** (Figure 4). Note that our experiments have no direct means to quantify to what extent **ii** isomerizes to **ii2** prior to decomposition to styrene and atomic hydrogen. However, by a comparison with the related cyano radical–ethylene reaction, we can present a qualitative trend. In the latter reaction, the authors deduced that the hydrogen migration from the initial $NCCH_2CH_2$ radical intermediate to $NCCHCH_3$ accounts for less

(49) Kaiser, R. I. *Chem. Rev.* **2002**, *102*, 1309–1358.

(50) Steinfeld, J. I.; Francisco, J. S.; Hase, W. L. *Chemical Kinetics and Dynamics*; Prentice Hall: Upper Saddle River, NJ, 1999.

(51) *NIST Chemistry WebBook*; Linstrom, P. J.; Mallard, W. G., Eds.; National Institute of Standards and Technology: Gaithersburg, MD, 2003.

(52) Blanksby, S. J.; Ellison, G. B. *Acc. Chem. Res.* **2003**, *36*, 255–263.

(53) Kaiser, R. I.; Mebel, A. M. *Int. Rev. Phys. Chem.* **2002**, *21*, 307–356.

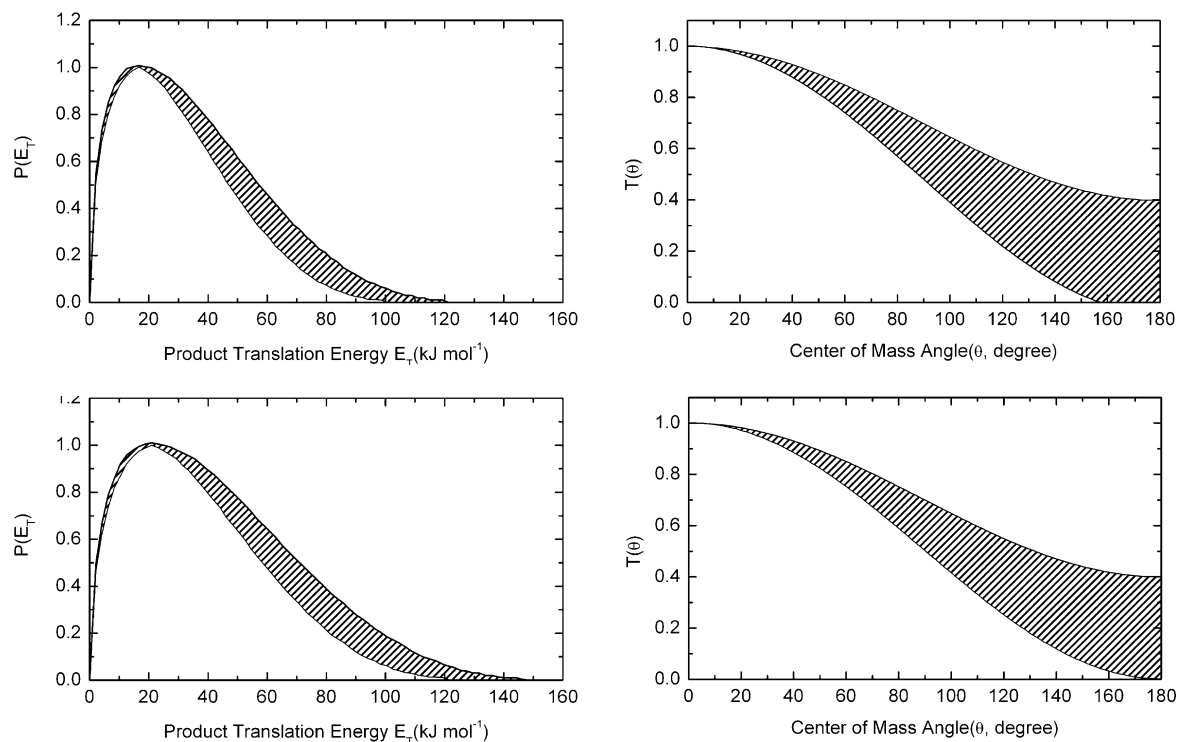


FIGURE 3. Center of mass translational energy (left) and angular distributions (right) for the reaction of phenyl plus ethylene to form C_8H_8 plus atomic hydrogen for two collision energies of 83.6 (upper) and 105.3 kJ mol^{-1} (lower).

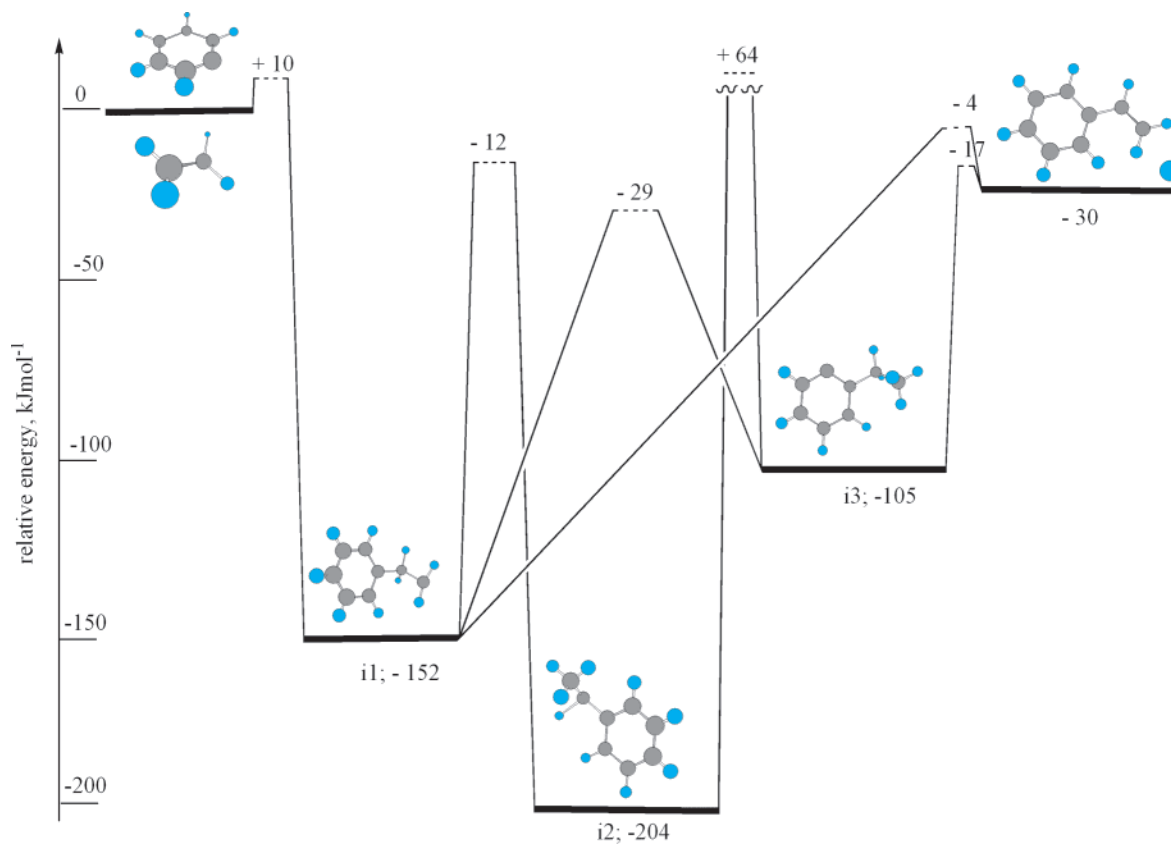


FIGURE 4. Schematic representation of potential energy surface (PES) involved in the reaction of phenyl radicals with ethylene leading to styrene (phenylethylene) plus atomic hydrogen extracted from ref 40. The carbon and hydrogen atoms are denoted in black and blue, respectively.

than 10% of the scattering signal of the vinyl cyanide (C_2H_3-CN) plus atomic hydrogen reaction product. This reaction was

carried out at much lower collision energies of only 15.3 kJ mol^{-1} and 21.0 kJ mol^{-1} compared to the phenyl–ethylene

TABLE 1. Peak Velocities (v_p), Speed Ratios (S), Center-of-Mass Angles (Θ_{CM}), Together with the Collision Energies (E_c) of the Reactants^a

beam	v_p , ms ⁻¹	S	E_c , kJ mol ⁻¹	Θ_{CM}
C ₂ H ₄ (X ¹ A _g)	896 ± 10	15.0 ± 1.0	-	-
C ₆ H ₅ (X ² A ₁)/He	2709 ± 57	5.3 ± 0.2	83.6 ± 3.2	6.9 ± 0.2
C ₂ H ₄ (X ¹ A _g)	921 ± 25	15.0 ± 1.0	-	-
C ₆ H ₅ (X ² A ₁)/He	3067 ± 34	6.0 ± 0.3	105.3 ± 2.6	6.2 ± 0.3
C ₂ D ₄ (X ¹ A _g)	897 ± 12	15.0 ± 1.0	-	-
C ₆ H ₅ (X ² A ₁)/He	2995 ± 121	6.1 ± 0.5	111.0 ± 8.3	7.3 ± 0.3

^a Note that the peak velocities and corresponding speed ratios refer to those segments of the pulsed beams which are crossing in the interaction region.

reaction; also, the center-of-mass angular distribution of the CN–C₂H₄ system was only mildly forward-peaked at higher collision energy. An enhanced collision energy is expected to reduce the probability of a hydrogen migration prior to the decomposition of the reaction intermediate. Therefore, we may conclude that in case of the phenyl–ethylene reactions, the rearrangement from **i1** to **i2** plays only a minor role in the reaction dynamics. We would like to comment briefly on the possible role of the intermediate **i3**. The latter can isomerize to **i2** via a barrier located about 64 kJ mol⁻¹ above the separated reactants. Although this transition state can be passed, based on the collision energies of our experiments, the back-reaction of **i3** to **i1** presents a more favorable route because of the energetically preferred transition state. Finally, the previous computations proposed bicyclic reaction intermediates which either ring-open and/or emit hydrogen atoms.³⁷ However, these pathways are highly endoergic, a finding not verified by our experiments. Most important, these pathways would also lead to an emission of deuterium atoms in the reactions of D₄-ethylene with phenyl. This has not been observed in our experiments either. Therefore, we may conclude that the involvement of bicyclic reaction intermediates and reaction products resulting from ring-opening mechanisms of the phenyl ring are unimportant.

Conclusions

In this study, we investigated the chemical dynamics of the reaction of phenyl radicals, C₆H₅, with ethylene, C₂H₄, under single collision conditions at two collision energies. Our data indicated that the reaction was indirect via complex formation and involved an addition of the phenyl radical to the olefinic bond of the ethylene molecule forming a C₆H₅CH₂CH₂ intermediate. The latter was found to decompose via a tight exit transition state to yield the styrene molecule (C₆H₅C₂H₃) plus atomic hydrogen. The overall reaction was found to be exoergic by 25 ± 12 kJ mol⁻¹. Experiments with D₄-ethylene demonstrated that the phenyl moiety stayed intact. Our study provides solid evidence that in combustion flames and in the circumstellar envelopes of carbon rich stars such as IRC+10216 and planetary nebulae like CRL 618,⁵⁴ the styrene molecule, a crucial precursor to form polycyclic aromatic hydrocarbons (PAHs), can be synthesized within a single neutral–neutral collision, a long-standing theoretical prediction which has remained to be confirmed by laboratory experiments under well-defined conditions until now.

Experimental Section

The experiments were carried out under single collision conditions in a crossed molecular beam machine at The University of Hawai'i.^{55,56} A pulsed supersonic beam of phenyl radicals was generated by flash pyrolysis of nitrosobenzene (C₆H₅NO) at seeding

fractions of less than 0.1% in the primary source chamber employing a modified Chen source⁵⁷ coupled to a piezoelectric pulsed valve.⁵⁸ Here, 3040 Torr helium gas (99.9999%) was guided into a stainless steel reservoir, which contains the solid nitrosobenzene sample at 283 K. The mixture was expanded at a stagnation pressure of 920 Torr through a resistively heated silicon carbide tube. By using helium as a calibration gas, the temperature of the tube was estimated to be around 1200–1500 K. The pulsed valve was operated at 200 Hz with pulses 150 μs wide. At these experimental conditions, the decomposition of the nitrosobenzene molecule to form nitrogen monoxide and the phenyl radical is quantitative. After passing a skimmer, a four-slot chopper wheel sliced a component of the phenyl radical beam with peak velocities v_p between 2709 and 3067 ms⁻¹ (Table 1). Number densities of the phenyl radicals in the interaction region of the main chamber were estimated to be a few 10¹³ radicals cm⁻³. The phenyl radical beam intersected neat and pulsed ethylene (99.999%) and D₄-ethylene (+99% D) beams released by a second pulsed valve at a pressure of 550 Torr under well-defined collision energies; the peak velocities and speed ratios of those segments of the hydrocarbon beams interacting with the phenyl radical beam are compiled in Table 1. Note that the D₄-ethylene experiment was carried out to pin down the position of the hydrogen/deuterium atom loss, i.e., an emission from the ethylene versus the phenyl moiety.

The reactively scattered products were monitored using a quadrupole mass spectrometric detector in the time-of-flight (TOF) mode after electron-impact ionization of the molecules at 90 eV. The detector could be rotated within the plane defined by the primary and the secondary reactant beams to take angular resolved TOF spectra in steps of 1.5°/2.0°. By integrating the TOF spectra at distinct laboratory angles, the laboratory angular distribution, i.e., the integrated signal intensity of an ion of distinct m/z versus the laboratory angle, could be extracted. Information on the chemical dynamics was gained by fitting these TOF spectra and the angular distribution in the laboratory frame (LAB) using a forward-convolution routine.^{59–61} This approach initially assumed an angular distribution $T(\theta)$ and a translational energy distribution $P(E_T)$ in the center-of-mass reference frame (CM). Since the previous kinetic studies of phenyl radical reactions with unsaturated hydrocarbons showed the existence of a threshold energies to reaction, E_0 ,^{32,37} we incorporated an energy dependent cross-section, $\sigma(E_c) \sim [1 - E_0/E_c]$, via the line-of-center model with the collision

(54) Cernicharo, J.; Heras, A. M.; Tielens, A. G. G. M.; Pardo, J. R.; Herpin, F.; Guelin, M.; Waters, L. B. F. M. *Astrophys. J.* **2001**, *546*, L123–L126.

(55) Gu, X.; Guo, Y.; Kawamura, E.; Kaiser, R. I. *J. Vac. Sci. Technol., A* **2006**, *24*, 505–511.

(56) Guo, Y.; Gu, X.; Kawamura, E.; Kaiser, R. I. *Rev. Sci. Instrum.* **2006**, *77*, 034701/034701–034701/034709.

(57) Stranges, D.; Stemmler, M.; Yang, X.; Chesko, J. D.; Suits, A. G.; Lee, Y. T. *J. Chem. Phys.* **1998**, *109*, 5372–5382.

(58) Kohn, D. W.; Clauberg, H.; Chen, P. *Rev. Sci. Instrum.* **1992**, *63*, 4003–4005.

(59) Kaiser, R. I.; Ochsenfeld, C.; Stranges, D.; Head-Gordon, M.; Lee, Y. T. *Faraday Discuss.* **1998**, *109*, 183–204.

(60) Vernon, M. Ph.D., University of California, Berkeley, 1981.

(61) Weiss, M. S. Ph.D., University Of California, Berkeley, 1986.

energy E_C for $E_C \geq E_0$ in the fitting routine.⁶² Recall that no reliable data on the *collision-energy dependence* of the cross-section exist; in this case, the line-of-center model is often utilized as a simplified model. TOF spectra and the laboratory angular distribution were then calculated from these center-of-mass functions. Because of the low signal counts, we had to accumulate up to 3.2×10^6 TOF spectra to obtain a reasonable signal-to-noise ratio of the reactively

(62) Levine, R. D. *Molecular Reaction Dynamics*; Cambridge University Press: Cambridge, 2005.

scattered species. This limited us to conduct the experiment with the D4-ethylene reactant only by recording TOF spectra at the center-of-mass angle.

Acknowledgment. This work was supported by the US Department of Energy, Basic Energy Sciences (DE-FG02-03ER15411). We would also like to thank Ed Kawamura (University of Hawaii, Department of Chemistry) for assistance.

JO071006A